MAPPING OF COMPOSITIONAL ANOMALIES IN AGGLUTINATES ON THE LUNAR SURFACE.

L. V. Starukhina[1], Yu. G. Shkuratov[1], V. V. Omelchenko[1], C. M. Pieters[2], [1]Astronomical Institute of Kharkov National University, Sumskaya 35, Kharkov, 61022. Ukraine; [2]Brown University, Providence, RI 02912 USA, starukhina@astron.kharkov.ua

Introduction: Composition of mare and highland agglutinites was shown to be slightly shifted to the average between that of mare and highland [1], similar to the shift observed for regolith samples as compared to the local bedrocks [2]. Mare agglutinitic glasses are Al-enriched and depleted of Fe, Ti, and Cr, whereas highland ones are depleted of Al and enriched in Fe, Ti, and Cr. This suggests global mixing processes that affect predominantly the particles most exposed to the space environment, i. e. agglutinates [1]. Such processes, namely, transport of dust and atoms via the lunar exosphere, were considered in [3,4]. Here we continue the simulation of the regolith compositional evolution mapping agglutinate compositional anomalies on the lunar surface.

Maps of agglutinate composition anomalies: Detailed compositional and spectral analyses of lunar soils carried out by the Lunar Soil Characterization Consortium (LSCC) [e.g., 5] give a unique opportunity to develop a technique that might be successfully used in remote compositional analysis of the lunar surface. The analysis supplies us with chemical data not only for bulk samples, but also for mineral components including agglutinates. We used the LSCC data to find relationships that provide the highest correlation coefficients between various linear combinations, $\log(P) = aA_{415} + bA_{750} + cA_{900} + dA_{1000}$, of albedo A (in %) at Clementine UVVIS spectral bands and the parameter P that presents the abundance of a mineral or chemical element [6]. We have found the coefficients of the linear combinations (Table 1) for agglutinate content (in %), bulk (total) abundance of FeO and Al_2O_3, and abundance of FeO and Al_2O_3 in agglutinates. The corresponding correlation coefficients are also presented in Table 1. Then we make prognosis maps for the mentioned parameters using Clementine UVVIS data.

Table 1.	*a*	*b*	*c*	*d*	*e*	*k*
Agg. cont	-0.062	0.04	-0.063	0.052	1.776	0.84
FeO	-0.063	0.102	0.029	-0.112	1.376	0.89
FeO agg.	-0.116	0.107	-0.008	-0.04	0.888	0.83
Al_2O_3	0.052	-0.082	-0.046	0.107	0.991	0.86
Al_2O_3 agg.	-0.006	-0.029	-0.169	0.191	0.961	0.74

In Fig.1 the map of the ratio of Al_2O_3 in agglutinates to total Al_2O_3 percentage is presented, in Fig.2 the same for FeO is shown; both maps are normalized by agglutinate content. As one can see in Figs.1 and 2, mare agglutinates are enriched in Al_2O_3 and depleted in FeO as compared to the bulks, whereas the agglutinates on highlands the opposite relation is observed. As can be anticipated in both these cases the highest anomalies are observed for young craters and their ray systems.

Chemical composition evolution of regolith particles: Change in chemical composition of fine particles (<10 μm) occures in two processes. (1) Loss of surface atoms in sputtering by solar wind protons and evaporation of target material in micrometeorite impacts and deposition of atoms that were sputtered or evaporated at distant sites. (2) Contamination of the upper regolith layer by high-velocity dust ejecta from distant craters. As dust particles that cover mare-highland distances have speed ~1 km/s, they penetrate in the regolith to some depth. Thus so only a part of high-velocity dust ejecta contribute to agglutinate particles. Following [3,4], global deposition flux of sputtered and evaporated atoms can be estimated as $8\text{x}10^5$ cm^{-2}s^{-1}, or $3\text{x}10^{-17}$ g·cm^{-2}s^{-1}. Among the sputtered atoms, heavier elements are preferentially deposited [3,4], so in atomic mixing, the abundance of Fe increases as compared to its abundance in the regolith composition averaged over the Moon. This average composition (21.8 wt.% Al_2O_3 and 7.3 wt.% FeO) is the limit point for mixing by the dust mechanism. Total flux of globally distributed dust was estimated with the mass spectra for small impactors [7], taking crater-to-projectile diameter ratios from [8,9]. The fraction of dust that takes part in global transport was calculated using the ejecta velocity distributions from [10,11]. The resulting flux of dust amounts equals $1.1\cdot10^{-16}$ g·cm^{-2}s^{-1} (or $3\cdot10^{6}$ cm^{-2}s^{-1}), ≈40% of it being due to the ejecta from microcraters on particle surfaces.

The best fit with the compositional trends on Al_2O_3-FeO plane from [1] is obtained, if ≈60% of globally distributed dust enter into agglutinates, i.e., for atoms to dust mass ratio ≈1:2. In Fig. 3 the simulated trends are shown. The total time scale is of the order of that found in [12] for total exposure time for a fine particle on the regolith surface ($1.5\cdot10^5$ years). The modeling show that the ratios of the final Al_2O_3 and FeO contents to their initial contents for mare and highland particles are about the same, as is obtained for mare and highland areas in Figs.1 and 2.

Conclusions: Maps of prognosis of bulk and agglutinate composition of the lunar regolith were obtained using the technique proposed in [6]. This technique uses LSCC and Clementine data. Simulation of the chemical evolution of a regolith particle exposed to lunar exosphere and to fine dust particles of ejecta have shown that this mechanisms of global mixing can account for the compositional anomalies observed for agglutinitic glasses [1] and obtained for the entire lunar surface.

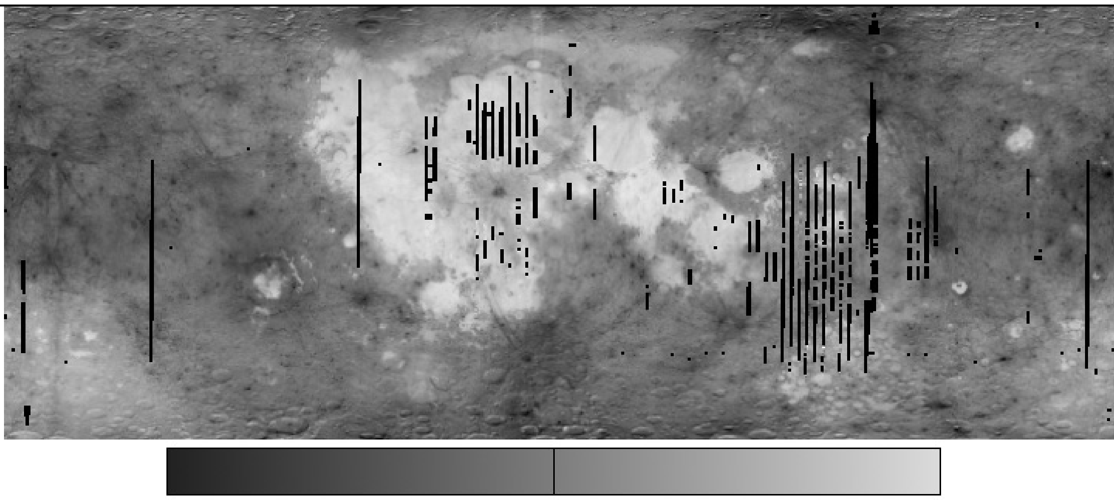

Fig. 1. Al_2O_3(agg.)/(Al_2O_3(total)·agg)

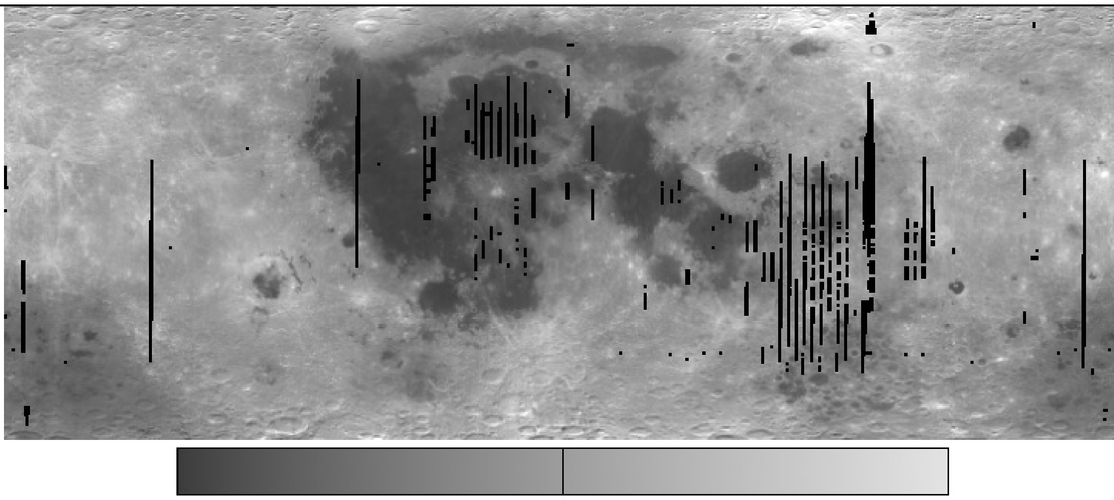

Fig. 2. FeO(agg.)/(FeO(total)·agg)

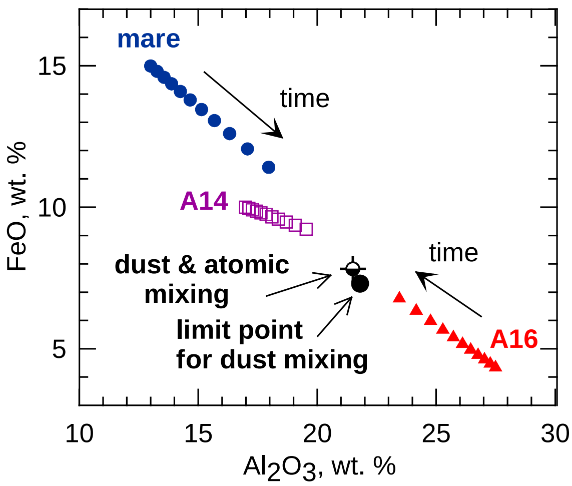

Fig. 3. Simulation of the evolution of composition of 10 μm regolith particles; initial and final points of the trends correspond to those in (Pieters, Taylor, 2003), total time intervals are 330 thousand years.

References: [1] Pieters C., Taylor L. (2003) *Geophys. Res. Lett. 30(0)*, doi: 10.1029/2003 GL 08212. [2] Haskin L., Warren P. (1991) *Lunar Sourcebook*. N.Y, 1991, 357-474. [3] Starukhina L. (2003) *Solar Syst. Res.*, *37*, 36-50. [4] Starukhina L. and Shkuratov Yu. (2004) *LPSC XXXV*, Abstr. # 1497. [5] Taylor L. et al. (2001). JGR. E106, 27,985 – 28,000. [6] Shkuratov Yu. et al. (2003) JGR. Planets. 108. (E4). 1-1 – 1-12. [7] Lebedinets V. (1981) *Aerosol in the upper atmosphere and cosmic dust*. Leningrad, Hydrometeoizdat. [8] Basilevsky A. T. et al. *Impact craters on the Moon and planets* Nauka, Moscow, 1983. [9] Vedder J., Mandeville J.-C. (1974) JGR. *79*, 3247-3256. [10] Ivanov B. A. (1976) *Proc. Lunar Sci. Conf. 7th*, 2947-2965. [11] Melosh, H. (1989) *Impact cratering: A geologic process*. Oxford Univ. Press, N.Y., 1989. [12] Borg J. et al. (1976) *Earth Planet. Sci. Lett.*, *29*, 161-174.